

Compressively Pre-stressed Navy Relevant Laminated and Sandwich Composites Subjected to Ballistic Impact

Eric Kerr-Anderson, Selvum Pillay, Basir Shafiq, and Uday K. Vaidya

Abstract Assembled structures such as ship decks, walls, and masts are often times under different degrees of pre-stress or confinement. Structural composite integrity can be compromised when subjected to impacts from events such as wave slamming, tool drops, cargo handling, and ballistic fragments/projectiles. It has been shown by several researchers that when a highly pre-stressed structure is subjected to impact, the damaged area and impact response changes. The main focus of this study was the impact of compressively pre-stressed structures which can also be considered as compression-during-impact. The results showed that for various laminate configurations, there was a compressive pre-stress threshold above which impact damage caused more damage than witnessed in typical compression after impact (CAI) tests. Both fiberglass and carbon laminates pre-stressed to higher than 30% of ultimate compressive strength, failed from impact at 300 m/s; but the carbon laminates developed shear cracks above 10% of the ultimate compressive strength. The work is of benefit to naval and other composite designers to be able to account for failure envelopes under complex dynamic loading states, i.e. pre-stress and impact for various composite configurations.

Book chapter for paper presented at Office of Naval Research (ONR) Workshop/Conference, June 23–24, 2011, Institut Clement Ader (ICA), Toulouse, France, Organized by – Serge Abrate, Bruno Castanié and Yapa D.S. Rajapakse.

E. Kerr-Anderson • S. Pillay • U.K. Vaidya (✉)
Materials Processing and Applications Development (MPAD) Composites Center,
Department of Materials Science & Engineering, University of Alabama at Birmingham,
Birmingham, AL 35294, USA
e-mail: uvaidya@uab.edu

B. Shafiq
Department of Engineering, University of Puerto Rico at Mayaguez,
Mayaguez, PR, USA

Keywords Sandwich composites • High velocity impact • Pre-stress • Compression

1 Introduction

Composite structures continue to replace steel structures on naval vessels in order to create lighter and often more cost effective structures. Fiberglass offers operational accessibility that steel and aluminum cannot compete with due to the near elimination of maintenance costs. Steel naval vessels must undergo extensive inspection and maintenance regiments each year while in a corrosive marine environment. Attempts have been made to reduce the weight of some steel naval vessels by replacing steel components with aluminum, which resulted in costly maintenance and replacement. The high cyclical swaying loading provided by ocean waves caused severe stress corrosion to develop in the aluminum structures. Large cracks formed over short periods of time which resulted in fracture. An additional drawback of aluminum has been the drastic structural strength loss during fires. Fiberglass naval vessels have been widely used as minecountermeasure vessels in which typical construction methods included the use of a framed single skin design, an unframed monocoque design, and a sandwich hull utilizing a thick polyvinyl chloride (PVC) foam core. The 73 m long Visby class corvette was the first naval ship to incorporate large amounts of carbon fiber into its hull which is comprised of a hybrid carbon and glass fiber polymer laminate covering a PVC foam core. Some designs range in weight savings between 20 and 60%. The reduction of weight allows for better performance in the form of speed or reduced fuel consumption. The reduction of weight also provides additional cargo or payload capacity. Other benefits include radar and magnetic transparency; yielding stealthier ships less susceptible to prevalent magnetic mine attacks [1]. A comprehensive understanding is required to establish optimal weight savings in terms of damage caused by blast waves, ballistic impact, and fire. This study examined the synergistic effect of compressive pre-stress and impact to determine if load bearing structures would be able to withstand ballistic impact.

Laminated and sandwich composites are susceptible to impact damage from events such as tool drops, wave impacts, bullets/fragments, and log debris strikes to name a few [1–3]. The impact damage typically follows a conical profile illustrated in Fig. 1 primarily in the form of matrix cracking, fiber breakage and delamination in a laminated composite.

The well-defined impact regimes for laminated composites are – low velocity impact (LVI), intermediate velocity impact (IVI), high velocity impact (HVI), and hyper velocity impact (HPI) [2–4]. LVI covers the broadest forms of impact usually involving a large mass (1–10 kg) impacting at relatively low velocities (<10 m/s). LVI events represent accidental tool drops, cargo falling, or other non-static loading scenario. IVI events typically occur between 10 and 100 m/s which range from rock debris to lower energy fragments. HVI or ballistic impact typically involves small mass projectiles, such as a 2 g 7.62 mm diameter steel sphere, traveling at high

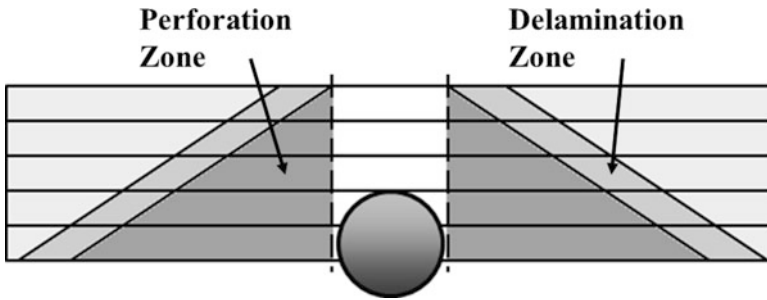


Fig. 1 Energy absorbing failure modes of ballistic impact on woven laminated composite structures

velocities (> 100 m/s). HVI events include ballistic impacts, fragment, shrapnel, and debris impact [5]. HPI represents small mass meteorites impacting at velocities in excess of 2,000 m/s. The differences between the four classes are based on impact velocity, mass, and contact area which translates into imparted strain and momentum exchange deformation.

For a normal impact event with constant mass and contact area, the impact force, damage evolution, resultant strains and stresses of the target laminate are highly dependent on the impactor velocity. LVI to a laminate may cause out-of-plane deflection, but minimal fiber breakage. Most damage in this mode is in the form of matrix shearing between lamina, i.e. delamination. As the impact velocity increases, the delaminated area extends outward in a conical shape from the point of impact through the thickness to the distal face and fiber breakage may be more prevalent. The lowest velocity at which the entire thickness delaminates and the projectile penetrates the laminate is called the ballistic limit or V_{50} . As the velocity is increased further, the initial layers of material begin to shear and delamination begins afterwards, which in effect shifts the conically shaped delamination zone to an inverse funnel. If the laminate is sufficiently rigid, a high enough impact velocity causes a shear plug, leaving a relatively clean hole with little or no delamination [2–4]. It has also been observed that the conical delamination angle for a globally rigid laminate is much less than that of a somewhat flexible laminate.

Compression after impact (CAI) is one of the standard test methods to determine residual strength after impact [6–8]. It is a means to determine the compressive strength after an impact event. There have been three main CAI fixtures developed by NASA, Boeing, and Airbus. The NASA CAI test utilizes a sample with dimensions $10\text{--}12.5 \times 7 \times 0.25$ in. for low velocity impact after which the sample is trimmed to $10\text{--}12.5 \times 5 \times 0.25$ for compression testing [6]. The NASA fixture has no accommodation for thickness variation and uses a large amount of material. The Boeing fixture, which has been adopted as ASTM D 7137 [7], requires test samples 6 in. long by 4 in. wide and a thickness between 4 and 6 mm. The Boeing test fixture allows the most sample dimension flexibility as the thickness can be adjusted, but it provides only a simply supported contact on all edges. The side supports have a knife edge support to allow bending while the top and bottom clamps are square to

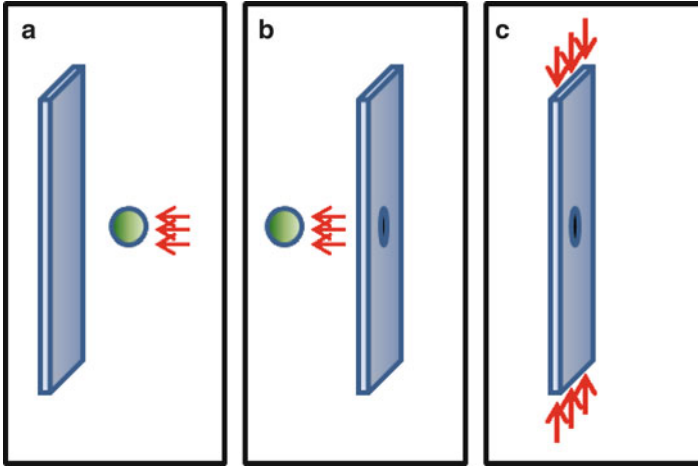


Fig. 2 Standard compression after impact (CAI) test; (a, b) sample is impacted, and (c) impacted sample is compressed to failure

prevent brooming. The top and bottom supports are not clamped but press fit at best. The Airbus CAI fixture utilizes a sample with dimensions 6 in. \times 4 in. \times 4 mm, and allows for a fully clamped top and bottom while providing a simply supported side constraint. There is no accommodation for thickness variation, but the Airbus fixture does incorporate the top support into the main fixture to force alignment, which is not accounted for with the Boeing CAI fixture. Additionally there have been some scaled up versions of the Boeing CAI test fixture to accommodate samples up to 10.5 \times 10.5 in. and with longer aspect ratios as much as 17 \times 4 in. [8]. All CAI data in this study was obtained using a CAI fixture consistent with ASTM D 7137 specifications. The samples are large enough to account for the damage area caused by the impact event, the sides of the sample are simply supported, and the ends are supported to prevent brooming. Figure 2 below illustrates the process of obtaining a CAI test result.

With the CAI test method, samples are impacted (Fig. 2a, b) and compressed to failure in a CAI fixture (Fig. 2c). Since no in-plane load is applied until after the impact event, no synergistic effects between impact and compression can be extrapolated from the CAI test. However, structural components are under pre-load during an impact event, which is the reason for observation of pre-stress effects during impact.

Assembled structures such as ship decks and walls are oftentimes under different degrees of compression pre-stress or confinement [9]. When a pre-stressed structure is subjected to impact, this condition can be considered as compression-during-impact (CDI). Although this is a more complex test to conduct, the results are more representative of in-field condition. Figure 3 shows the difference between CAI and CDI.

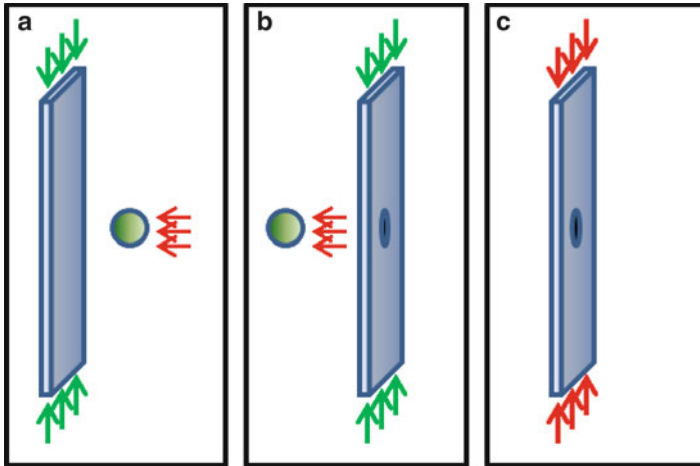


Fig. 3 Pre-stressed compression during impact (CDI) test method – (a) pre-stress is applied; (b) pre-stressed sample is impacted, and (c) impacted sample is compressed to failure

CDI testing involves compressing a sample prior to impact (Fig. 3a), impacting the sample (Fig. 3b), and compressing the damaged sample to failure in the CAI fixture (Fig. 3c). For both methods step (c) is the same.

Since structural composite materials are susceptible to impact events, it is important for design purposes to characterize the extent of damage caused by impact. Naval designers must be able to account for failure envelopes under a complex loading state. Several researchers have examined the residual strength after impact event to accommodate the loss in structural properties due to any anticipated impact from service use. The methods used to obtain design allowables have included residual flexural strength after impact (FAI), tensile strength after impact (TAI), compression strength after impact (CAI), strain energy density calculations, and impact under pre-stressed conditions.

Testing of impact under pre-stressed conditions requires $5\times$ more samples than CAI testing and requires an additional 20 min per sample for installation and pre-stressing. It is preferable to have experiments replicate service conditions as close as possible to ascertain synergistic effects of loading and impact, which can be otherwise missed from post-testing an impacted sample under tension, compression, or flexure.

Lamination theory is adequate to predict failure in tension and flexure for most laminated systems [10, 11]. However, compressive strength for composite laminates has been more difficult to characterize, because models are idealized, and require difficult to attain properties. For example, it has been reported that in-plane compressive strength of a composite material can be less than a tenth of the in-plane tensile strength [11–13]. Most fiber reinforcements have a small fiber diameter (8–22 μm) to obtain enhanced tensile, bending, and torsional properties. Smaller diameters are detrimental to compressive loading. Since classical Euler buckling is directly related to the second moment of inertia, each small diameter fiber has a

very low buckling strength when compared to its tensile strength. When loaded in compression, the fibers begin to buckle and compress the matrix. The fibers begin to fail when the matrix yields and a critical buckling radius is reached.

2 Impact of Laminated Composites

There have been numerous studies of impact on composite structures. Several models have been implemented based on analytical methods [14–27]. Naik et al. [5] explored the shift in energy absorbing mechanisms when altering the impact velocity of a projectile. They confirmed that the highest amount of energy is absorbed at the ballistic limit, and proposed a momentum exchange model. Hazell et al. [24] reported that even at very high velocities (1,825 m/s) there appeared to be an asymptotic maximum delamination area threshold. Several studies have reported the impact face distortion caused at the impact contact area. In some cases, this distortion affects through the thickness profile [5, 16, 22–27].

In a pre-stress composite laminate, the momentary geometrical distortion caused by a point impact can cause it to behave differently due to the local strains causing geometrical distortion. The compressive buckling load is lower due to the increased out of plane deflection. Several approaches used to enhance compression performance under impact include: increasing interfacial strength, increasing matrix yield strength, or decreasing the global deflection with ribbing or other reinforcing methods.

One of the main methods used to determine laminate properties after an impact event is to use a standard tensile, compression, or flexural test on impacted samples. Trudel-Boucher et al. [28] examined the effects of LVI damage on the residual flexural and tensile strengths of 3.5 mm thick cross-ply glass fiber/polypropylene composites. They observed that damage progressively increased as the impact energy increased, and at the highest impact energy of 9 J plastic deformation resulted in residual curvature. They also reported that both the normalized flexural strength and modulus decreased linearly with respect to the impact energy. Applying flexure on the non-impacted side resulted in higher flexural strength, but resulted in a pronounced drop in flexural modulus. This indicated that compression was a limiting factor for flexural strength.

Trudel-Boucher et al. [28] also showed that the normalized tensile strength was not affected until an impact energy greater than 5 J was reached, after which it decreased. The tensile modulus was not affected by the level of impact damage. O'Higgins et al. [29] suggested that insight into the damage evolution for impacted tensile specimens can be obtained from investigating the crack initiation and growth in an open hole tension test. It was seen that cracks propagated transversely from the hole until failure. It was also seen that the stress concentration decreased as higher levels of damage were attained, which resulted in higher open hole tensile

strength. Craven et al. [30] modeled a carbon/epoxy multi-directional laminate with pre-existing damage patterns under tensile loading and observed its effect on the tensile stiffness. It was found that both delamination and fiber fracture cracks must be taken into account to determine residual tensile properties. Cui et al. [31] modeled a T300/BMP-316 laminate in which tensile specimens were subjected to LVI prior to applying tensile load to capture the effect of actual damage instead of crack concentrations. The transverse crack forms at the boundaries of the delaminated zone and then propagates outward until failure. The error associated with this method for both damage area and residual tensile strength was less than 10%.

3 Residual Strength of Laminated Composites

There have been numerous studies on the residual compressive strength after impact of composite laminates, because impact damage can reduce the residual compressive strength to as low as one tenth the ultimate strength for carbon/epoxy and one third for E-glass/epoxy laminates. Several authors have shown that decrease in compressive strength is directly correlated to the impact damage area. Since the impact damage area is highest at the ballistic limit, the compressive strength decreases as a function of impact velocity, and reaches an asymptotic value at the ballistic limit. CAI samples are first impacted which forms the frustum shaped damage area associated with non-pre-stressed impact shown in Fig. 1. The impact damage causes a stress concentration to form with the applied compressive load at the edge of the delaminated area perpendicular to the applied load. It has been shown that a linear elastic fracture mechanics approach can be used to determine limiting loads that cause crack growth [2, 32]. Shear cracks propagate outward from the point of impact quickly to the edge of the delaminated area, then slowly continue to propagate until catastrophic failure occurs. Gillespie Jr. et al. [33] showed that stitching of sandwich panels and cross-ply laminates created marginal improvements in the CAI strength. Zhou et al. [34, 35] examined preconditioned laminates with embedded films to replicate delamination damage. Oval, rectangular, and circular delaminations were created at multiple locations through the thickness of the laminate. Comparisons were made between open hole, impact damaged and preconditioned residual compressive strengths.

Several authors have researched the CAI strength of sandwich composites, where several additional failure modes occur associated with the core. Williams et al. [36] used a modified CAI fixture and CFRP laminates containing hollow glass fibers filled with uncured resin. Samples were impacted, subjected to a curing cycle to heal the damaged area, and residual strengths were obtained using a CAI test. The study concluded that an impacted laminate could retain a majority of its original strength via this method. Aoki et al. [37] showed that hygrothermal conditions can drastically affect the CAI strength. The wet samples had a lower T_g than dry samples, and when CAI was conducted above the T_g of the matrix, compressive properties dramatically

decreased. This study indicated that the yield strength of the matrix has a dominant effect on the compressive strength of a laminate.

4 Strain Rate Sensitivity

When characterizing damage caused by an impact event, the determination of strain rate sensitivity for a material is critical. Daniel et al. [38], Xiao et al. [39], and Brown et al. [40] have conducted strain rate sensitivity studies on composite laminates and observed that, as the strain rate increases, the modulus and strength increase, but the strain to failure decreases. LS-DYNA's MAT 162 [41] utilizes strain rate sensitive strength and modulus functions as given by:

$$\{S_{RT}\} = \{S_0\} \left(1 + \frac{C_{Rate} \ln\{\dot{\epsilon}\}}{\dot{\epsilon}_0} \right) \quad (1)$$

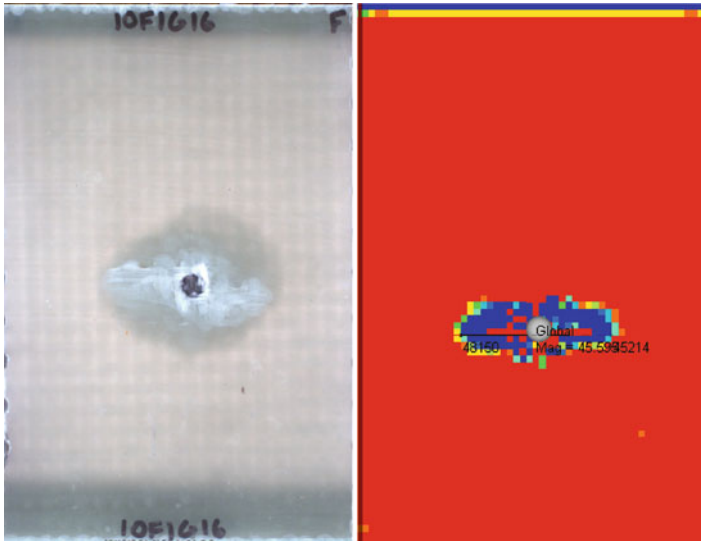
$$\{E_{RT}\} = \{E_0\} \left(1 + \frac{C_{Rate} \ln\{\dot{\epsilon}\}}{\dot{\epsilon}_0} \right) \quad (2)$$

where the rate coefficient is a user defined input used to fit data regressions. Based on the work done by Matzenmiller et al. [42], this method is important for pre-stressed materials, because although the initial loading is quasi-static the impact event and initial failure upon impact is a dynamic event. As discussed by Abrate [2], the shear, compressive, and tensile waves produced at an impact site repeatedly travel back and forth through the laminate, prior to any distortion. When failure takes place, the recoil force causes damage at a higher strain rate than the loading rate. The result of which is a laminate failing at a lower strength than anticipated from standard residual strength test methods. Preliminary studies by the authors have shown that the strain sensitivity functions of MAT 162 can be used to effectively model the impact under compression damage as shown below in Figs. 4 and 5.

The resultant front face damage area of a fiberglass laminate pre-stressed to 190 MPa impacted by a 2 g 7.62 mm diameter steel sphere at 120 m/s had an 8.8% error between the experiment and model, for the front face crack length.

5 Impact Under Pre-load

Several researchers examined impact while under a pre-load. These investigations include – analytical models, FEA, biaxial loading under impact, compression under impact, torsion/shear under impact, flexure under impact, and tension under impact. Sun and Chattopadhyay [43] studied central impact of a mass on a simply supported plate. They analytically determined that the contributions of pre-



Figs. 4 and 5. Pre-stressed impact damage area of experimental (*Left*) compared with the finite element analysis (*Right*)

stressed tension on an impacted composite reduced the deflection, bending stress, shear force, and energy absorption due to impact. Rossikhin and Shitikova [44] used a ray series approximation and linearized Hertzian contact deformation to analytically determine the effect of in-plane compressive pre-stressed orthotropic circular plates under normal low velocity impact. It was analytically shown that a compressive pre-stress will soften the impact response and cause greater out-of-plane deflection. It was shown that shear locking occurs at the compressive critical magnitude, which attenuates the transverse shear wave similar to Landau attenuation witnessed in highly compressed gases. Zheng and Binienda [45] analyzed laminated plates which were simply supported and impacted using a linearized elastoplastic contact law and shear deformable plate theory. The contact force history was not affected by prestress, but it was found that pre-stress significantly affected the out-of-plane deflection. Pre-tension reduced the deflection and pre-compression increased deflection. Rossikhin and Shitikova [46] went on to determine the impact response generalized non-dimensional equations for transversely isotropic plates with compressive pre-stress. It was found that as the compressive force increased due to impact, the shear wave was attenuated. The concentrated absorbed energy was closer to the impact site which caused more damage. The studies showed that additional compressive pre-stress caused more deflection and less contact force.

Schoeppner and Abrate [22] examined the Air Force Research Laboratory (AFRL) database and found that for AS4/3501-6 graphite/epoxy laminates subjected to a tensile pre-load up to $2,400 \mu\epsilon$ and impacted up to 4.2 m/s caused no significant difference in the delamination threshold limit. Khalili et al. [47] used

Sveklo's elastic contact theory to determine analytical results for an impact under both uniaxial and biaxial tensile pre-stress. It was determined that the maximum impact force increased and central deflection increased as the tensile pre-load increased. For the unidirectional carbon fiber laminate analyzed, the transverse pre-stress caused more of the aforementioned effects than the longitudinal pre-stress. Biaxial pre-stress resulted in the most impact force increase and central deflection decrease. Garcia-Castillo et al. [48] conducted a study in which the ballistic limit of 1.5 mm thick aluminum samples was determined in the unloaded and 38% pre-loaded tensile state. There was no discernible difference in the ballistic limit, but it was witnessed that the pre-loaded samples catastrophically failed upon impact while the unloaded samples did not fail.

Minak et al. [49, 50] investigated carbon fiber epoxy cylinders which were pre-stressed in torsion prior to LVI. They reported that the torsional pre-load did not change the delamination initiation though it aids in the delamination propagation. High torsional pre-load resulted in more delamination propagation, lower critical buckling loads, and lower residual torsional strength. Catastrophic failure resulted in some cases. Mizukawa et al. [51] created a fixture which allowed torsion and bending to be applied to thin walled tubes while being impacted by a drop tower. They found that there was a synergistic effect between the apparent torsional stress and apparent bending stress when under impact. Kepler and Bull [52] conducted tests on sandwich panels subjected to global bending while ballistically impacted. They found that under applied bending loads, the impact caused catastrophic shear cracking that was non-existent without the applied bending. Kulkarni et al. [53] conducted a drop tower study on plain woven fiberglass samples which were pre-stressed by pressurizing the distal side of the laminate up to 0.9 MPa. No discernible difference was witnessed in the range of pre-stress tested.

Robb et al. [54] conducted drop tower studies on biaxially pre-loaded chopped E-glass polyester laminates. It was found that the most damage, least contact force, and least contact duration were caused in a biaxially loaded tension/compression state. Tensile pre-stress caused stiffening while compressive pre-stress caused softening. Whittingham et al. [55] tested carbon fiber epoxy laminates under realistic biaxial pre-stressed loads witnessed in the field. It was found that within the realistic biaxial pre-stressed state, no discernible difference was witnessed. Mitrevski et al. [56] examined the effect of impactor shape on the biaxially pre-stressed impact of E-glass/polyester laminates. As the contact surface of the impactor shifts from cylindrical to spherical to conical, the maximum deflection and absorbed energy increased. At the levels of pre-tensioned biaxial impact tested, no discernible differences of damaged area were observed. Garcia-Castillo et al. [57] conducted studies on woven glass/polyester laminates subjected to high velocity normal impact under both uniaxial and biaxial tensile pre-stress. It was determined that the biaxially preloaded samples had a slightly higher ballistic limit, but for the range of preload tested there were no discernible differences in the energy absorbing terms of primary yarn, secondary yarn, kinetic energy cone, delamination, and matrix cracking. Loktev [58] studied spherical impact on a pre-stressed orthotropic Uflyand-Mindlin plate using a Legendre polynomial and Laurent series expansion. It

was determined that pre-tensioned samples had a higher contact force and duration, while the pre-compressed laminates had a lower contact force and duration. A positive pre-stressed moment caused a stiffening response and dramatically reduced the contact duration.

Finite element model (FEM) analysis has been conducted on the impact response on pre-stressed laminates. Mikkor et al. [59] used PAM-CRASH to analyze ballistic failure of pre-stressed laminates. Their findings show that at higher tensile pre-stress, failure occurs higher than a critical impact velocity. Choi et al. [60, 61] examined in-plane pre-stress with the FEM method and experimental results to determine that tensile pre-stressed caused a faster impact response while compressive pre-stress induced a slower response. Ghelli and Minak [62] studied the effect of membrane pre-loads through FEA. It was shown that tensile pre-load increased the peak stress while the compressive pre-load reduced the peak impact stress.

Herzl Chai [63] conducted LVI testing on stiffened carbon/epoxy panels pre-stressed in compression. A 0.5 in. diameter aluminum sphere impacted the pre-stressed laminates up to 400 fps. It was determined that shear cracks leading to catastrophic failure developed at 30% of the ultimate compressive strength. Equations were derived based on a strain energy density analysis which accurately modeled the failure phenomenon of impact under compression. McGowen and Ambur [64] conducted compressive pre-stressed impact on graphite/epoxy sandwich panels with honeycomb cores. Similar results were achieved as Chai in which pre-stressed samples caused failure upon impact at high levels of pre-stress. Zhang et al. [65] also compressed laminates prior to impact and found that failure can result if the compressive pre-stress is too high during impact. Varying buckling shapes at impact were compared. Herszberg and Weller [66] conducted studies for impact under compressive pre-loads on stitched and unstitched carbon/epoxy laminates. Catastrophic failure was also found at high pre-stress levels when impacted. Stitching was found to dramatically reduce the impact damage area, though it had no effect on the penetration velocity or catastrophic failure thresholds. Heimbs et al. [67] impacted compressively pre-stressed carbon/epoxy laminates and observed catastrophic failure witnessed by the aforementioned researchers. The quasi-isotropic laminates exhibited damage reshaping as pre-stressed conditions increased. Additionally LS-DYNA was used to corroborate the results. Pickett et al. [68] conducted a study using a significantly longer sample to apply in-plane compressive pre-stress during drop tower impact. The carbon/epoxy laminates exhibited transverse cracks when impacted at high pre-stress. PAM-CRASH was used to validate the witnessed failure modes.

Wiedenman and Dharan [69] investigated samples of G10 glass of varying thicknesses compressed to different levels and penetrated with a 5.56 mm projectile with the equivalent of an M4 carbine. A CAI fixture and portable MTS load frame were used to apply in-plane compressive load. It was found that the combination of impact and compressive strain was much more detrimental than that of impact alone. They also observed a delamination reshaping to damage more of the structure perpendicular to loading and shear kink band formation due to impact. There was no account for the increased deflection which would be present in thinner samples.

The authors found good agreement when using the model presented by Starnes et al. [70].

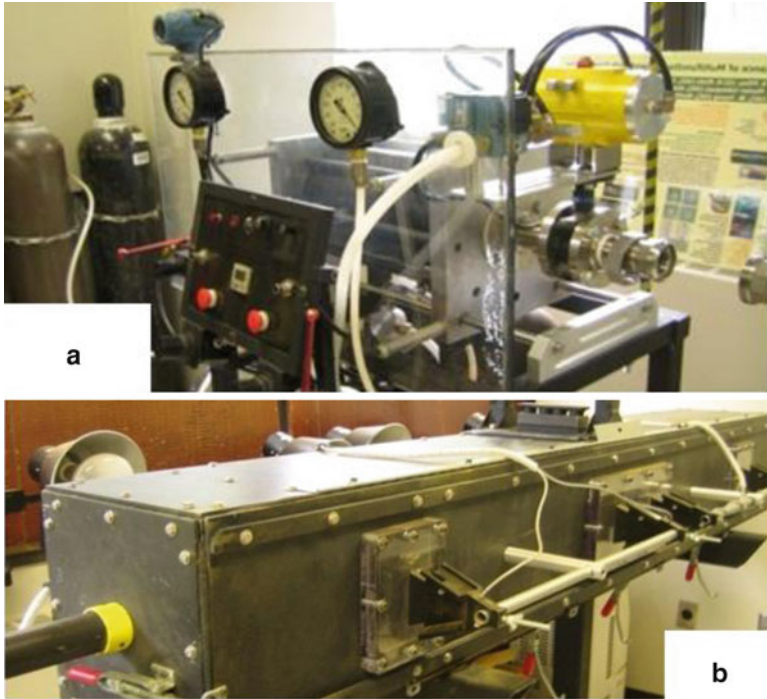
The database for complex loading of polymer matrix composites is sparse. Predictive models have been implemented with some success to help fill the gap for the lack of test data, but to truly understand the failure strength of a laminate configuration a large amount of exploratory testing must be conducted. Testing conducted closest to the service loading witnessed at failure would yield more accurate failure thresholds and allow existing models to be supplemented. The work done on pre-stressed composites by the authors provides additional insight into failure modes that could be witnessed by structural composites subjected to an impact event. By understanding the failure mechanisms and failure thresholds, improved predictive models can be developed for use by naval designers. The value to naval designers would be the reduction of required safety factors by removing some of the uncertainty associated with complex loading. A reduced safety factor would allow for an optimized structure, which by further reducing vessel weight would result in increased naval vessel performance.

6 CDI Fixture Design

For the purpose of evaluating realistic residual strength after impact, studies were conducted by the authors to characterize the synergistic effect of impact under pre-stressed in-plane compression for woven glass/vinyl ester (VE) composite laminates. The ballistic impact equipment used was a custom built gas gun allowing for spherical ball rounds up to 12.7 mm (0.5 in.) diameter to be fired up to 350 m/s. The equipment illustrated in Figs. 6 and 7 and 7 uses compressed helium to propel a machined foam sabot housing a projectile down the barrel [71]. The sabot breaks apart when it strikes the stripper plate and the projectile continues to propel to the sample. Velocity measurements were attained from two sets of Oehler Model 35 proof chronographs with the Oehler Skyscreen III photo detectors.

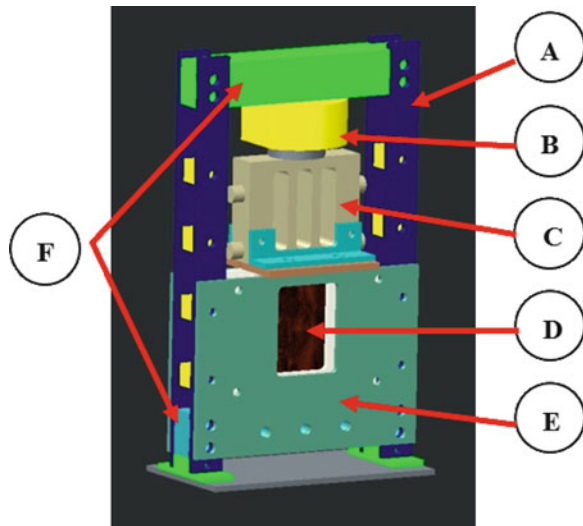
The compression during impact (CDI) fixture used to conduct pre-stressed testing was designed, machined, and manufactured in-house, see Fig. 8. The CDI fixture fits inside the capture chamber dimensions of 304 mm × 292 mm × 100 mm (12" × 11.5" × 4"). It is completely replaceable when required, and effectively applies uniform, in-plane compressive loads of up to 300 kN. Load is applied with a 30 t low-clearance hydraulic cylinder as shown in Figs. 8 and 9. The hydraulic cylinder used was a manually operated unit retrofitted with both a psi gage and a pressure transducer which allowed monitoring of the applied load before and after impact.

All of the components of the CDI fixture are attached with bolts. The fixture was designed so that the hydraulic cylinder was placed outside the capture chamber, and a load transfer block is used to both apply load to the sample and mimic the clamped end condition used in the CAI test fixture. The samples are constrained in-plane by two adjustable ½" plates shown in Fig. 9, which allowed a slip-fit to be



Figs. 6 and 7 Gas Gun (a) and (b) Capture Chamber

Fig. 8 CDI fixture. A: vertical support bars, B: hydraulic cylinder, C: load transfer block, D: sample, E: front and back support plates, F: top and bottom support bars



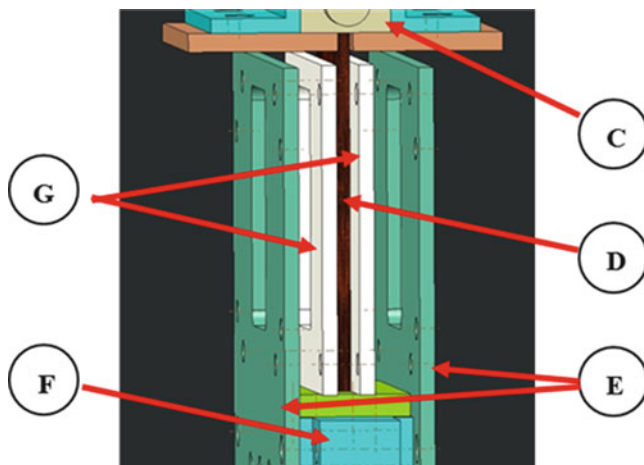


Fig. 9 Side view of CDI fixture – C: load transfer block D: sample, E: front and back support plates, F: bottom support bar, and G: inner slip-fit support plates

achieved. The bottom and top support bars are made from 2 in. square steel bars, and an exchangeable contact plate is used to provide for testing flexibility.

7 Procedure and Material

Samples were made via a VARTM process and machined to 4" × 6" rectangular samples for CDI testing. Samples were installed in the CDI fixture and a load was applied. The sample was given at least 30 s to relax prior to impact. All samples in this study were impacted with a 0.3 in. steel sphere weighing 2 g at velocities ranging from 75 to 350 m/s. After impact, the load was released, backlit photography was adopted, and samples were compressed to failure in an ASTM CAI fixture. Samples tested included 6 mm thick woven orthotropic E-glass/VE laminates, 4.2 mm thick woven orthotropic E-glass/VE laminates, 6.2 mm thick quasi-isotropic E-glass/VE laminates, sandwich panels made of 3.1 mm thick quasi-isotropic E-glass/VE face sheets with a 50.8 mm thick HP 130 divinyl cell foam core, and 3.4 mm thick orthotropic carbon fiber/VE laminates.

8 Results and Discussion

The effect of compressive pre-stress on the residual strength of a 6 mm thick E-glass/VE composite laminate is shown in Fig. 10 [72]. Each series represents the level of in-plane compressive pre-stress the laminate was subjected to when im-

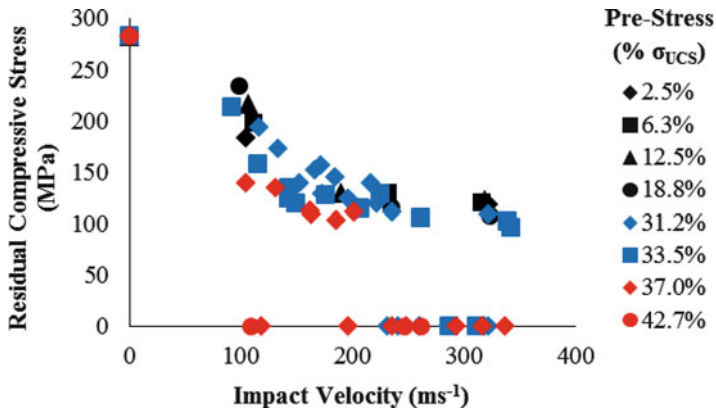


Fig. 10 Effect of compressive pre-stress on residual strength after impact

packed. Five samples tested in accordance with the Combined Loading Compression (CLC) ASTM D6641 [73] yielded an ultimate compressive strength, σ_{UCS} , of 377 (± 40) MPa.

At higher loading levels (31.2, 33.5, 37.0, and 42.7% σ_{UCS}), samples failed compressively when impacted at velocities higher than 225 m/s. These samples are displayed along the x-axis of Fig. 10, since their residual strength was zero. These samples failed because the impact event damaged enough material where the remaining cross-sectional area was unable to sustain the applied load. The effect of changing the geometrical loading of compression due to the instantaneous out of plane distortion caused by the impact event causes this failure. The point at 0 m/s was determined from baseline compression tests of unimpacted samples using the CAI fixture. The baseline compressive strength found using the CAI fixture was 280 MPa, which was much less than the ultimate compressive strength obtained from CLC testing. The CLC fixture [73] utilizes a much shorter span length of 12.7 mm and larger grip lengths of 64 mm in comparison to the CAI fixture [7] which has a span length of roughly 137 mm and grip lengths of 8 mm. The CAI fixture does not adequately constrain samples to be used for determining ultimate compressive strength.

Statgraphics [69] was utilized to determine empirical best-fit regression. The correlation was in found to fit the form:

$$\sigma_{Residual} = 0.75\sigma_{UCS} - B\sqrt{(V_{Impact})} \quad (3)$$

The model indicates that the residual compressive strength can be derived by subtracting from the compressive ultimate strength, B , times the square root of the impact velocity. The coefficient B which is unique to each loading level is derived from the constituents of the sample and the amount of pre-stress. Each regression passed an ANOVA analysis with a 95% confidence level. The comparison of these

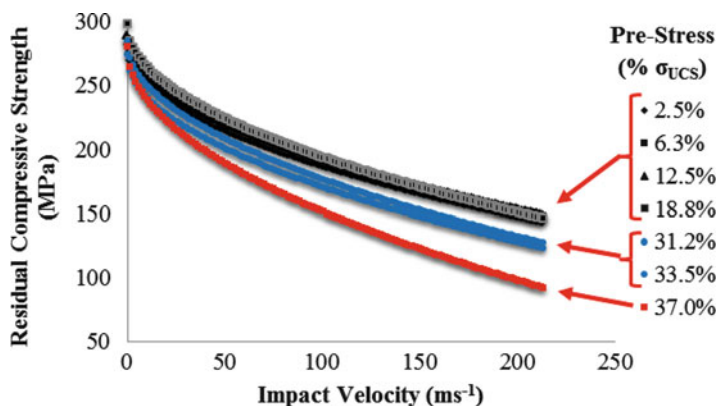


Fig. 11 Effect of pre-stress on residual strength after an impact (regression line comparison)

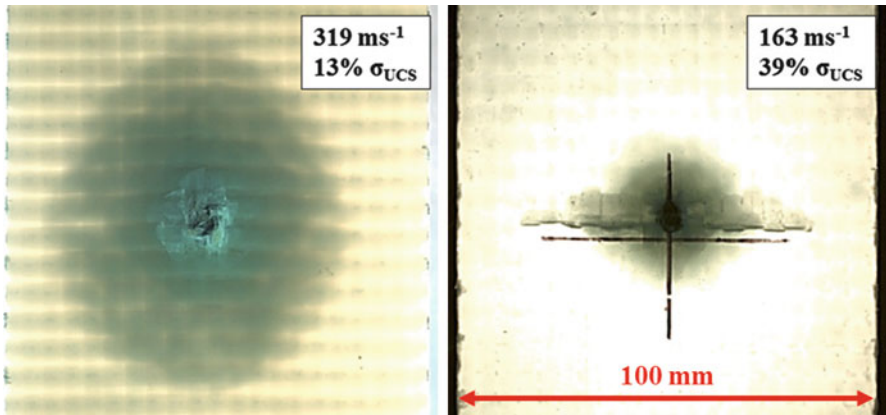
regressions, as seen in Fig. 11, indicated that there is little statistical difference in the first four loading levels. Residual strength decreased as the loading increased in the range of 31% up to 37%, which implied that there was an increase in transverse cross-sectional damage.

Regressions were only plotted up to 225 m/s due to the failure witnessed at higher impact velocities. The pre-stress level of 42.7% was not plotted, because all samples failed due to impact. This drop in residual strength was observed to be due to an impact induced shear crack (IISC) on the front face of the laminate. The IISC was similarly seen in studies by Kepler et al., Chai, and Wiedenman et al. [48, 59, 65]. The length of the IISC increased with increase in impact velocity as illustrated in Figs. 12 and 13. It was also observed that as the IISC increased in length, the delamination area increased. With increase in IISC, an additional conical delamination zone develops whose base is in the front face of the composite. This base is elliptical in nature following the profile of the IISC. For nominally thick laminates – such as 4 mm or greater for woven glass/VE, the total delamination area resembles a distorted yo-yo or an hourglass on its side.

The damage evolution resulting in a set of glass/VE laminates from increasing the impact velocity and compressive pre-stress is shown in Fig. 14. The lighter images are back-lit samples showing the delamination damage. The darker images are front lit samples showing the formed IISC. All pictures are at the same magnification. Impact velocity increases from top to bottom, and compressive pre-stress increases from left to right in the figure.

The formation of an IISC is clearly visible for the higher pre-stressed samples, and failure can be seen at high compressive pre-stress and at higher loading combinations.

By plotting the residual strength as a function of the length of the compression initiated crack in Fig. 15, a strong correlation is obtained linking the front face crack length to a decrease in the residual strength (i.e. cross-sectional area). A further



Figs. 12 and 13 Development of a front face crack due to high pre-stress. (Left) displays a typical conical delamination zone; (Right) shows a developing conical delamination zone with the addition of an IISC on the Front Face

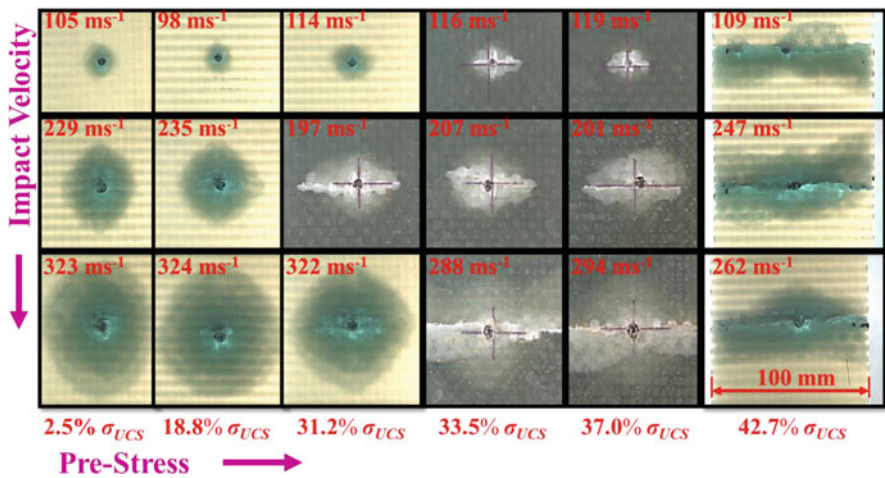


Fig. 14 Evolution of damage from increased compressive pre-stress during ballistic impact

ANOVA analysis validated the correlation. When the crack length becomes too large, the sample fails in compression.

Since the crack length directly correlates with the residual strength, it is inferred that a front face crack denotes damage throughout the thickness of the composite. Figure 16 shows the samples failed due to impact. Failure was caused by a compressive pre-stress, but it was also observed that the synergistic effect of pre-stress and impact was more detrimental. Failure mode envelopes are observed in which typical conical damage occurs, an IISC is formed, and that IISC extends far

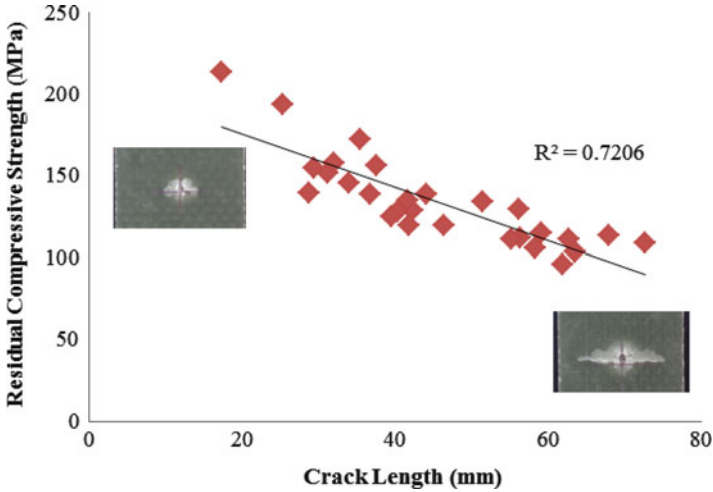


Fig. 15 Effect of front face IISC length on residual strength

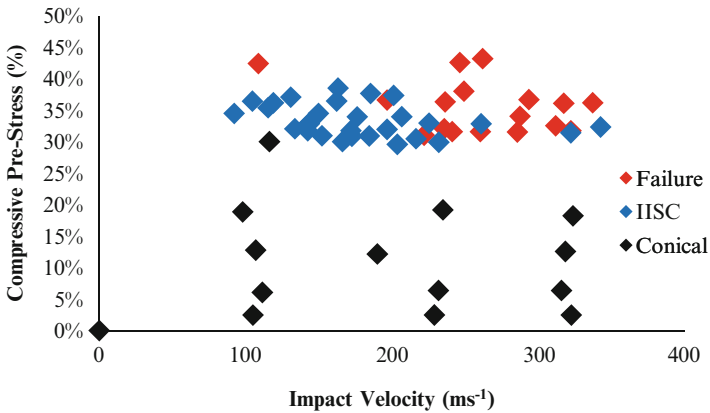


Fig. 16 Effect of compression and impact on failure mode type

enough to cause failure. The data from Fig. 16 is used to create failure threshold envelopes shown in Fig. 17.

These envelopes can be used to determine when it is safe to use predictive models for conical delamination, when additional safety factors may be needed, and when failure will occur.

Figure 18 is a contour plot displaying the combined effect of compression and impact on the residual compressive strength attained from CAI testing. Combined with the results from Figs. 11, 12, 13, 14, 15 and 16, it is seen that more transverse damage in the form of an IISC is created as a laminate is impacted under higher

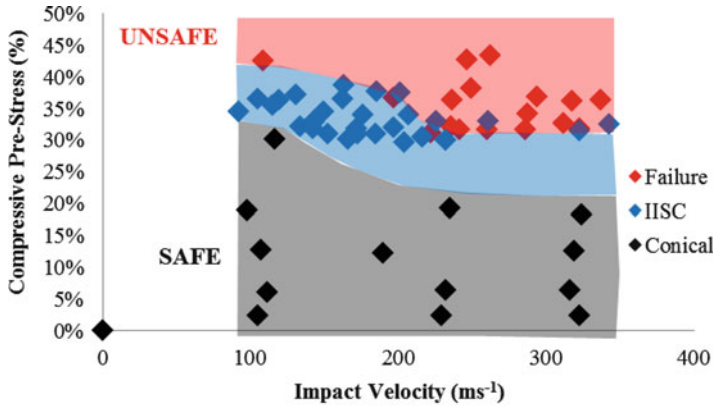


Fig. 17 Failure threshold envelopes

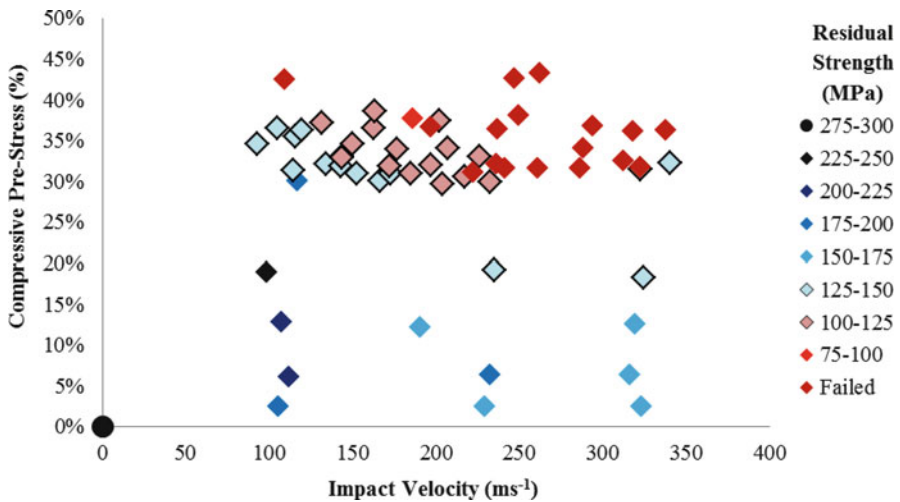


Fig. 18 Synergistic effect of compression and impact on the residual compressive strength of damaged GFRP

compressive pre-stress. For an impact velocity of 100 m/s, Fig. 18 displays that at low levels of compression there is very little change in the residual strength, but as the pre-stress is increased the residual strength reduces. Correlating these results with Fig. 17, it can be seen that the reduction in residual strength is directly linked with the formation of an IISC. The impact velocity also has a strong effect on the length of such a shear crack and the residual strength of the GFRP laminate.

Likewise, the penetration chart below in Fig. 19 designates the observed penetration of the compressed laminates. It was observed that for the samples tested thus far, none of the samples were fully penetrated at the tested impact velocities.

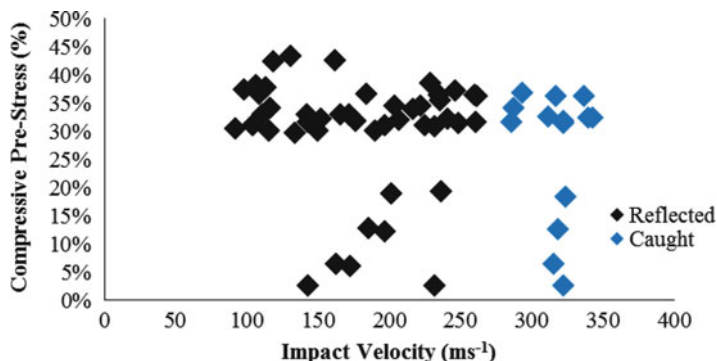


Fig. 19 Penetration chart for 100 mm × 150 mm (4'' × 6'') samples based on pre-stress and impact velocity

It may be noted that partial penetration only occurred at higher velocities. Based on the initial results, penetration does not seem to be effected by the synergistic effect of compression and impact indicating that the IISC formation occurs prior to penetration. Naik et al. have shown that the friction force between projectile and laminate absorbs significant amount of energy [5]. If the IISC had formed after penetration, more energy would be absorbed from the increased friction forces when pre-stress was applied and the ballistic limit decreases.

Similar studies have been conducted for other data sets including a 4.2 mm thick woven orthotropic E-glass/VE laminates, 6.2 mm thick quasi-isotropic E-glass/VE laminates, sandwich panels made of 3.1 mm thick quasi-isotropic E-glass/VE face sheets with a 50.8 mm thick HP 130 divinyl cell foam core, and 3.4 mm thick orthotropic carbon fiber/VE laminates [70]. The failure threshold envelopes associated with each of these data sets are shown below in Fig. 20.

The failure threshold envelopes remain relatively the same for E-glass/vinyl ester laminates. The carbon fiber data set showed a significant reduction in relative failure strength when compared to the E-glass fiber data set, which can be attributed to strain rate sensitivity associated with carbon fibers. Figure 21 shows the difference in damage evolution for the various data sets.

There was little difference between damage resulting in seven and ten layer orthotropic configurations. The $\pm 45^\circ$ contribution in the quasi-isotropic laminate displays damage biasing in both the delamination and IISC. The quasi-isotropic sandwich panel showed a more unique failure mode showing biased delamination and a thicker IISC.

Since the compressive modulus of the laminate facesheets and foam core differ and they are bound by a weaker interface, some barreling or tendency towards barreling occurs during loading. When the front laminate is impacted and penetrated, it is adequately supported by the core and associated impact deformation/delamination is reduced. The load carried by the delaminated front face is transferred to the surrounding undamaged material and the back laminate. The projectile is also

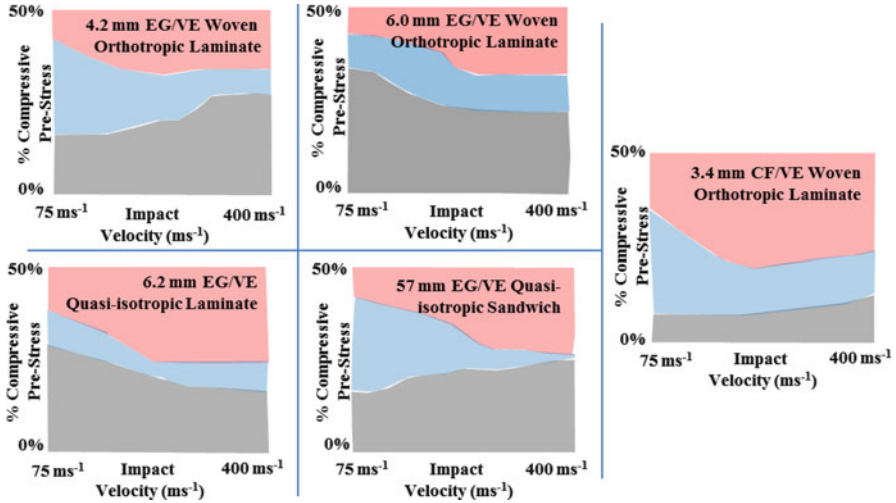


Fig. 20 Comparison of the failure threshold envelopes for various laminate configurations

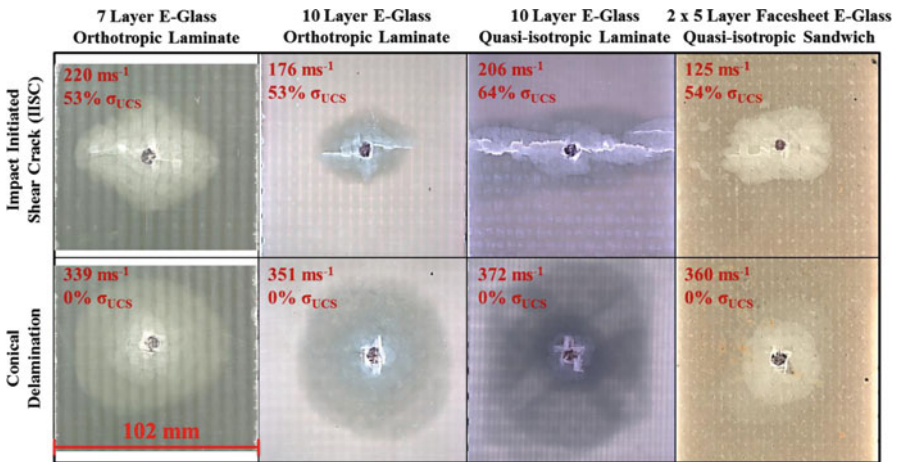


Fig. 21 Damage evolution effect of laminate configuration

significantly slowed down from penetrating the front facesheet. When the back facesheet is impacted, the projectile is moving slower which produces more damage if slightly less than the ballistic limit. The back facesheet is under a locally higher pre-stress due to the loss of structural integrity of the front facesheet. The back facesheet is also not supported by anything other than the interface and is essentially a five layer thick laminate with a much lower buckling load than the sandwich panel. All of these conditions lead to large delamination on the back facesheet. The structural failure associated with the back face damage is then passed back to the front which will force shear cracks to propagate if the stress concentration is

too high. Sandwich panels offer some of the most beneficial aspects for structural composites, but the addition of a foam core has many unintended consequences that must be accounted for during design.

It should be noted that many factors affect both compression and impact of composite structures to cause uncertainty. The information presented is intended as a guide to designers of what to expect to see when a structure is loaded too high and impacted. Considerable additional testing is required to be able to use such a threshold diagram for design purposes. The general trends have been established and presented by this and other works. Various factors have to be taken into account, such as percent strain, some span to thickness ratio, and percent ultimate stress to establish standard design guidelines for laminates impacted during compression.

9 Conclusion

This study provided some insights into the failure modes and safety thresholds of navy relevant composites in regards to ballistic impact when subjected to different degrees of in-plane compressive pre-stress. It was observed that beyond a threshold combination of impact velocity and degree of pre-stress, the shape of the damage changes from circular to elliptical leading to catastrophic damage. Failure was witnessed using the impact under compression test method which was not accounted for by standard CAI test methods. Failure envelopes for the combined effects of pre-stress and impact have been developed for orthotropic glass/vinyl ester laminates, quasi-isotropic glass/vinyl ester laminates, quasi-isotropic glass/vinyl ester sandwich composites, and carbon/vinyl ester laminates. Although the testing of the CFRP system was sparse, it indicated that a GFRP system would be better suited to structural application in compression, subject to ballistic impact. Since the ultimate compressive strength of a composite system is dependent on thickness, boundary conditions, and lay-up, it is difficult to pinpoint a safety threshold, but in this case the safety threshold for the orthotropic GFRP was 30% σ_{UCS} , quasi-isotropic GFRP was 40% σ_{UCS} , quasi-isotropic GFRP sandwich panel was 40% σ_{UCS} , and the orthotropic CFRP was 15% σ_{UCS} . Based on these results, the weight savings would not justify the use of the more expensive CFRP system for structural composites in an environment of ballistic threat. A significant amount of work is left to be done in this field relating to effectively modeling the residual strengths of pre-stressed impact for composite structures. A framework has been established to conduct such testing, but at present a constitutive model is yet to be developed.

Acknowledgements We are grateful to support from the ONR Solid Mechanics program managed by Dr. Yapa D.S. Rajapakse, Office of Naval Research. Some aspects of the compression fixture for crashworthiness studies were funded through the Department of Energy, Graduate Automotive Technology Education (GATE) program and we gratefully acknowledge this support.

References

1. Mouritz AP et al (2001) Review of advanced composite structures for naval ships and submarines. *Compos Struct* 53(1):21–42
2. Abrate S (1998) *Impact on composite structures*, 1st edn. Cambridge University Press, Cambridge
3. Vaidya UK (2011) Impact response of laminated and sandwich composites. *Courses Lect Int Cent Mech Sci* 526:97–192
4. Bartus SD, Vaidya UK (2005) Performance of long fiber reinforced thermoplastics subjected to transverse intermediate velocity blunt object impact. *Compos Struct* 67(3):263–277
5. Naik NK, Shirrao P (2004) Composite structures under ballistic impact. *Compos Struct* 66(1–4):579–590
6. NASA reference publication 1092 (1983) Standard tests for toughened resin composites. Langley Research Center, Hampton, Washington, DC: National Aeronautics and Space Administration pp 1–6
7. ASTM D 7137 (2005) Standard test method for compressive residual strength properties of damaged polymer matrix composite plates. American Society for Testing and Materials, West Conshohocken
8. Adams D (2007) Testing tech: compression after impact testing. *High-Performance Composites* Nov: 4–6
9. Critchfield M, Judy T, Kurzweil A (1994) Low-cost design and fabrication of composite ship structures. *Mar Struct* 7(2–5):475–494
10. Chamis CC, Lewis Research Center (1984) Simplified composite micromechanics equations for strength, fracture toughness, impact resistance and environmental effects. Lewis Research Center, Cleveland, NASA TM-83696
11. Agarwal BD, Broutman LJ, Chandrashekhara K (2006) *Analysis and performance of fiber composites*, 3rd edn. Wiley, Hoboken
12. Greenwood JH, Rose PG (1974) Compressive behaviour of kevlar 49 fibres and composites. *J Mater Sci* 9(11):1809–1814
13. Piggott MR (1981) A theoretical framework for the compressive properties of aligned fibre composites. *J Mater Sci* 16(10):2837–2845
14. Jones R et al (1993) Assessment of impact damage in composite structures. Department of Defence, Defence Science Technology Organisation, Aeronautical Research Laboratory, Fishermens Bend
15. Riedel W et al (2006) Hypervelocity impact damage prediction in composites: Part II—experimental investigations and simulations. *Int J Impact Eng* 33(1–12):670–680
16. Morye SS et al (2000) Modelling of the energy absorption by polymer composites upon ballistic impact. *Compos Sci Technol* 60(14):2631–2642
17. Li CF et al (2002) Low-velocity impact-induced damage of continuous fiber-reinforced composite laminates. Part I. An FEM numerical model. *Compos Part A* 33(8):1055–1062
18. He T, Wen HM, Qin Y (2007) Penetration and perforation of FRP laminates struck transversely by conical-nosed projectiles. *Compos Struct* 81(2):243–252
19. He T, Wen HM, Qin Y (2008) Finite element analysis to predict penetration and perforation of thick FRP laminates struck by projectiles. *Int J Impact Eng* 35(1):27–36
20. Tabiei A, Aminjikai SB (2009) A strain-rate dependent micro-mechanical model with progressive post-failure behavior for predicting impact response of unidirectional composite laminates. *Compos Struct* 88(1):65–82
21. Aymerich F, Dore F, Priolo P (2008) Prediction of impact-induced delamination in cross-ply composite laminates using cohesive interface elements. *Compos Sci Technol* 68(12):2383–2390
22. Schoeppner GA, Abrate S (2000) Delamination threshold loads for low velocity impact on composite laminates. *Compos Part A* 31(9):903–915

23. Duan Y et al (2006) A numerical investigation of the influence of friction on energy absorption by a high-strength fabric subjected to ballistic impact. *Int J Impact Eng* 32(8):1299–1312
24. Hazell PJ, Appleby-Thomas G (2009) A study on the energy dissipation of several different CFRP-based targets completely penetrated by a high velocity projectile. *Compos Struct* 91(1):103–109
25. Fujii K et al (2003) Effect of characteristics of materials on fracture behavior and modeling using graphite-related materials with a high-velocity steel sphere. *Int J Impact Eng* 28(9): 985–999
26. Sevkat E et al (2009) A combined experimental and numerical approach to study ballistic impact response of S2-glass fiber/toughened epoxy composite beams. *Compos Sci Technol* 69(7–8):965–982
27. Gama BA, Gillespie JW (2008) Punch shear based penetration model of ballistic impact of thick-section composites. *Compos Struct* 86(4):356–369
28. Trudel-Boucher D et al (2003) Low-velocity impacts in continuous glass fiber/polypropylene composites. *Polym Compos* 24:499–511
29. O’Higgins RM, McCarthy MA, McCarthy CT (2008) Comparison of open hole tension characteristics of high strength glass and carbon fibre-reinforced composite materials. *Compos Sci Technol* 68(13):2770–2778
30. Craven R et al. (2009) Buckling of a laminate with realistic multiple delaminations and fibre fracture cracks using finite element analysis. *ICCM Int Conf Compos Mater*
31. Cui H-P, Wen W-D, Cui H-T (2009) An integrated method for predicting damage and residual tensile strength of composite laminates under low velocity impact. *Comput Struct* 87(7–8):456–466
32. Elder DJ et al (2004) Review of delamination predictive methods for low speed impact of composite laminates. *Compos Struct* 66(1–4):677–683
33. Gillespie JW, Monib AM, Carlsson LA (2003) Damage tolerance of thick-section S-2 glass fabric composites subjected to ballistic impact loading. *J Compos Mater* 37(23):2131–2147
34. Zhou G, Rivera LA (2007) Investigation on the reduction of in-plane compressive strength in thick preconditioned composite panels. *J Compos Mater* 41(16):1961–1994
35. Zhou G (2005) Investigation for the reduction of in-plane compressive strength in preconditioned thin composite panels. *J Compos Mater* 39(5):391–422
36. Williams GJ, Bond IP, Trask RS (2009) Compression after impact assessment of self-healing CFRP. *Compos Part A Appl Sci Manuf* 40(9):1399–1406
37. Aoki Y, Yamada K, Ishikawa T (2008) Effect of hygrothermal condition on compression after impact strength of CFRP laminates. *Compos Sci Technol* 68(6):1376–1383
38. Daniel IM et al (2011) Characterization and constitutive modeling of composite materials under static and dynamic loading. *AIAA J* 49(8):1658–1664
39. Xiao JR, Gama BA, Gillespie JW (2007) Progressive damage and delamination in plain weave S-2 glass/SC-15 composites under quasi-static punch-shear loading. *Compos Struct* 78(2):182
40. Brown KA et al. (2007) Modelling the impact behaviour of thermoplastic composite sandwich structures. In: 16th International Conference on Composite Materials, ICCM-16 – “A Giant Step Towards Environmental Awareness: From Green Composites to Aerospace”, July 8, 2007 – July 13, 2007. International Committee on Composite Materials, Kyoto, Japan
41. LSTC, *LS-dyna user manual* 971, May 2007
42. Matzenmiller A, Lubliner J, Taylor RL (1995) A constitutive model for anisotropic damage in fiber-composites. *Mech Mater* 20(2):125–152
43. Sun CT, Chattopadhyay S (1975) Dynamic response of anisotropic laminated plates under initial stress to impact of a mass. *J Appl Mech* 42(3):693
44. Rossikhin YA, Shitikova MV (2006) Dynamic stability of a circular pre-stressed elastic orthotropic plate subjected to shock excitation. *Shock Vib* 13(3):197–214
45. Zheng D, Binienda WK (2008) Analysis of impact response of composite laminates under prestress. *J Aerosp Eng* 21(4):197–205

46. Rossikhin YA, Shitikova MV (2009) Dynamic response of a pre-stressed transversely isotropic plate to impact by an elastic rod. *J Vib Control* 15(1):25–51
47. Khalili SMR, Mittal RK, Panah NM (2007) Analysis of fiber reinforced composite plates subjected to transverse impact in the presence of initial stresses. *Compos Struct* 77(2): 263–268
48. García-Castillo SK, Sánchez-Sáez S, Barbero E (2011) Behaviour of uniaxially preloaded aluminium plates subjected to high-velocity impact. *Mech Res Commun* 38(5):404–407
49. Minak G et al (2010) Residual torsional strength after impact of CFRP tubes. *Compos Part B Eng* 41(8):637–645
50. Minak G et al (2010) Low-velocity impact on carbon/epoxy tubes subjected to torque – experimental results, analytical models and fem analysis. *Compos Struct* 92(3):623–632
51. Mizukawa K et al (1985) Impact strength of thin-walled composite structures under combined bending and torsion. *Compos Struct* 4(2):179–192
52. Kepler JA, Bull PH (2009) Sensitivity of structurally loaded sandwich panels to localized ballistic penetration. *Compos Sci Technol* 69(6):696–703
53. Kulkarni MD, Goel R, Naik NK (2011) Effect of back pressure on impact and compression-after-impact characteristics of composites. *Compos Struct* 93(2):944–951
54. Robb MD, Arnold WS, Marshall IH (1995) The damage tolerance of GRP laminates under biaxial prestress. *Compos Struct* 32(1–4):141
55. Whittingham B et al (2004) The response of composite structures with pre-stress subject to low velocity impact damage. *Compos Struct* 66(1–4):685–698
56. Mitrevski T et al (2006) Low-velocity impacts on preloaded GFRP specimens with various impactor shapes. *Compos Struct* 76(3):209–217
57. García-Castillo SK et al (2009) Impact behaviour of preloaded glass/polyester woven plates. *Compos Sci Technol* 69(6):711–717
58. Loktev AA (2011) Dynamic contact of a spherical indenter and a prestressed orthotropic uflyand-mindlin plate. *Acta Mech* 222(1–2):17–25
59. Mikkor KM et al (2006) Finite element modelling of impact on preloaded composite panels. *Compos Struct* 75(1–4):501–513
60. Choi I-H et al (2010) Analytical and experimental studies on the low-velocity impact response and damage of composite laminates under in-plane loads with structural damping effects. *Compos Sci Technol* 70(10):1513–1522
61. Choi I-H (2008) Low-velocity impact analysis of composite laminates under initial in-plane load. *Compos Struct* 86(1–3):251–257
62. Ghelli D, Minak G (2010) Numerical analysis of the effect of membrane preloads on the low-speed impact response of composite laminates. *Mech Compos Mater* 46(3):299–316
63. Chai H (1982) The growth of impact damage in compressively loaded laminates. PhD Dissertation. California Institute of Technology, Pasadena
64. McGowan DM, Ambur DR (1999) Structural response of composite sandwich panels impacted with and without compression loading. *J Aircr* 36(3):596–602
65. Zhang X, Davies GAO, Hitchings D (1999) Impact damage with compressive preload and post-impact compression of carbon composite plates. *Int J Impact Eng* 22:485–509
66. Herszberg I, Weller T (2006) Impact damage resistance of buckled carbon/epoxy panels. *Compos Struct* 73(2):130–137
67. Heimbs S et al (2009) Low velocity impact on CFRP plates with compressive preload: test and modelling. *Int J Impact Eng* 36(10–11):1182–1193
68. Pickett AK, Fouinneteau MRC, Middendorf P (2009) Test and modelling of impact on preloaded composite panels. *Appl Compos Mater* 16(4):225–244
69. Wiedenman N (2006) Ballistic penetration of compressively loaded composite plates. *J Compos Mater* 40(12):1041–1061
70. Starnes JH Jr, Rose CA (1997) Nonlinear response of thin cylindrical shells with longitudinal cracks and subjected to internal pressure and axial compression loads. In: Proceedings of the 1997 38th AIAA/ASME/ASCE/AHS/ASC Structures, Structural Dynamics, and Materials Conference. Part 4 (of 4), AIAA, Kissimmee, FL, 7–10 Apr 1997

71. Bartus SD(2006) Simultaneous and sequential multi-site impact response of composite laminates. PhD dissertation. University of Alabama at Birmingham, Birmingham
72. Vaidya U, Kerr-Anderson E, Pillay S (2010) Effect of pre-stressing and curvature on e-glass/vinyl ester composites, In: Proceedings mechanics of composite materials, College Park, MD
73. ASTM D 6641(2001) Standard test method for determining the compressive properties of polymer matrix composite laminates using a combined loading compression (clc) test fixture